The two-top molecule 3-penten-2-one: Acetyl methyl torsion in α,β-unsaturated ketones

Maike Andresen, Martin Schwell, Ha Vinh Lam Nguyen

The two-top molecule 3-penten-2-one: Acetyl methyl torsion in α,β-unsaturated ketones†

Maike Andresen,[a,b] Martin Schwell,[a] and Ha Vinh Lam Nguyen[a,c*]

[a] Univ Paris Est Creteil and Université de Paris, CNRS, LISA, F-94010 Créteil, France

[b] Institute of Physical Chemistry, RWTH Aachen University, Landoltweg 2, D-52074 Aachen, Germany

[c] Institut Universitaire de France (IUF), F-75231 Paris, France

† In memory of Wolfgang Stahl.

*Corresponding author. Email: lam.nguyen@lisa.ipsl.fr

Abstract

Using a molecular jet Fourier transform spectrometer, the microwave spectrum of *E*-3-penten-2-one, also called methyl propenyl ketone, was recorded in a range from 2.0 to 26.5 GHz. Two conformers, antiperiplanar (*ap*) and synperiplanar (*sp*), could be identified. Complicated splitting patterns arising due to the internal rotation of the acetyl methyl and propenyl methyl groups could be resolved, and all measured rotational transitions were fitted to measurement accuracy. The barrier heights of the acetyl methyl group are 434.149(37) cm^{-1} and 358.076(26) cm^{-1} for the *ap* and *sp* conformers, respectively. For the propenyl methyl group, the barrier is 581.903(45) cm^{-1} for the *ap* conformer and 595.271(71) cm^{-1} for the *sp* conformer. Comparing these results to those of other ketones categorized in a class system connecting the internal rotation of the acetyl methyl group to the structures of the molecules leads to an extension with a new class for α,β-unsaturated ketones.

Keywords: Rotational Spectroscopy, Microwave Spectroscopy, Large Amplitude Motion, Internal Rotation, Quantum Chemistry

Graphical Abstract

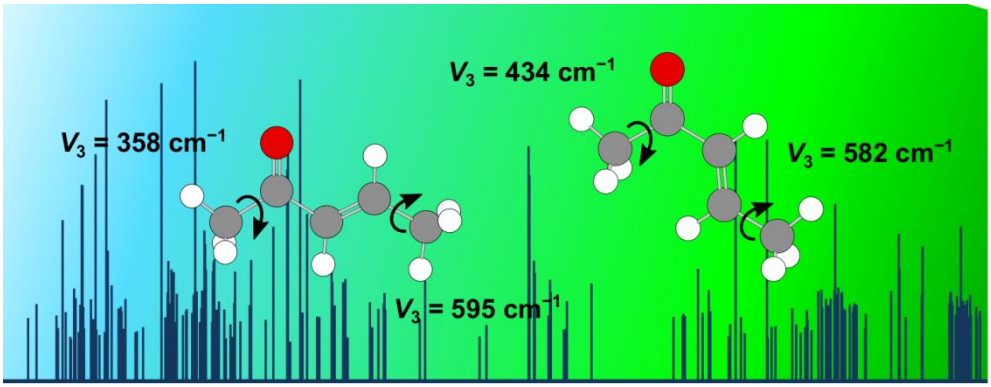

1. Introduction

Microwave spectroscopy is classically connected with the topic of structural chemistry, because the primary parameters deduced from a microwave spectrum, the rotational constants, directly reflect the mass distribution of the atoms in the molecule [1]. However, along the history of almost one century since the first microwave spectrum of ammonia was measured in 1934 [2], large amplitude motions (LAMs) have been involved, either in the form of inversion motion [3], ring puckering [4], or internal rotation [5]. If the molecule features a methyl group undergoing internal rotation, a torsional fine structure consisting of A-E doublets can be observed. If two methyl groups are involved, the fine structure becomes more complicated and appears in the form of quartets if the two methyl groups are equivalent, or quintets if they are not [6].

A link between the molecular structure and the torsional barrier of the acetyl methyl group in ketones has been reported in our previous work, and a classification system to categorize this phenomenon was introduced [7-10]. Observed conformers of a series of methyl *n*-alkyl ketones can be sorted in two classes based on their symmetry: the "C_s class" with barrier heights of about 180 cm^{-1}, and the "C_1 class" exhibiting barrier values of approximately 240 cm^{-1}. Herbers et al. proposed an additional "phenyl class" consisting of acetophenone and its derivatives with barriers ranging from 550 cm^{-1} to 630 cm^{-1}, which can probably be traced back to the phenyl ring attached on the other side of the carbonyl group [11]. Lastly, acetone [12], 1,1-difluoroacetone [13], and 1,1,1-trifluoroacetone [14] might form an "acetone class" with barrier heights of about 250 cm^{-1} [10].

Classifying unsaturated ketones in the above-mentioned categorization system is more complicated. In molecules like allyl acetone [15], where the double bond is located rather far away from the acetyl methyl group, no significant influence of the double bond on the barrier height is observed. Allyl acetone can be enclosed in the "C_1 class". However, when the double bond is in the α,β-position, like in methyl vinyl ketone [16] and ionone [17], it forms a π-conjugated system with the carbonyl group. Both molecules show two conformers, antiperiplanar (*ap*) and synperiplanar (*sp*), with the respective barrier heights of the acetyl methyl torsion being about 430 cm^{-1} and 350 cm^{-1}. Thus, these α,β-unsaturated ketones do not fit in any of the previous classes (C_s, C_1, phenyl, or acetone). In Ref. [10], we suggested a new class called the "mesomeric class". But since there are only two members in this class, methyl vinyl ketone [16] and ionone [17], the categorization is rather uncertain. Therefore, in the present work, we study 3-penten-2-one, also called methyl propenyl ketone, by a combination of microwave spectroscopy and quantum chemistry to expand the available data and to gain a better understanding of the proposed "mesomeric class".

3-Penten-2-one is a small unsaturated ketone with the molecular structure given in Figure 1, and a derivative of methyl vinyl ketone where a methyl group is added to the β-carbon atom. This methyl group –CH=CH–**CH_3**, called the propenyl methyl group, also undergoes internal rotation, making 3-penten-2-one a two-top case. Since the *Z* isomer are calculated to be about 9 to 18 $kJ \cdot mol^{-1}$ higher in energy and therefore not observable under our molecular jet measurement conditions, the present study will only focus on the *E* isomer of 3-penten-2-one.

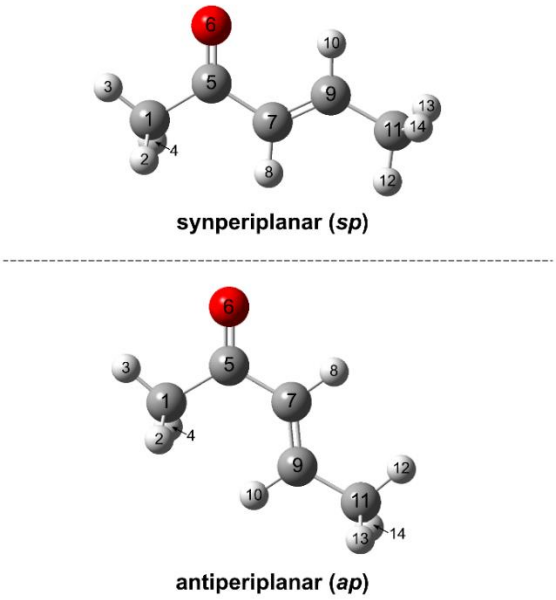

Figure 1: The two conformers of 3-penten-2-one as calculated at the MP2/6-311++G(d,p) level of theory. Hydrogen atoms are color-coded white, carbon atoms grey, and the oxygen atom is in red.

2. Quantum chemical calculations

2.1. Geometry optimizations

Different conformers of *E*-3-penten-2-one can be created by rotating the dihedral angle φ = $\angle(O_6,C_5,C_7,C_9)$, while changes of the dihedral angles α_1 = $\angle(O_6,C_5,C_1,H_3)$ and α_2 = $\angle(C_7,C_9,C_{11},H_{12})$ correspond to the internal rotations of the two methyl groups (for atom numbering see Figure 1). The conformational analysis was performed by changing φ from 0° to 180°, while all other geometry parameters were optimized at the MP2/6-311++G(d,p) and B3LYP-D3BJ/6-311++G(d,p) levels of theory using the *Gaussian 16* package [18]. A Fourier expansion with the terms summarized in Table S-1 in the Supplementary Material was used to parameterize the calculated energies. As shown in Figure 2, we obtained two minima, which were subsequently optimized under full geometry relaxation to yield the two conformers illustrated in Figure 1. Frequency calculations confirmed them to be true minima and not saddle points. Both conformers exhibit C_s symmetry and all heavy atoms are located in the C−(C=O)−C plane. According to the notation used for methyl vinyl ketone [16], the two geometries will hereafter be called the antiperiplanar (*ap*) and the synperiplanar (*sp*) conformers with the φ values being 180° and 0°, respectively. The rotational constants and dipole moment components of both conformers are listed in Table 1. Their nuclear coordinates are given in Table S-2 of the Supplementary Material.

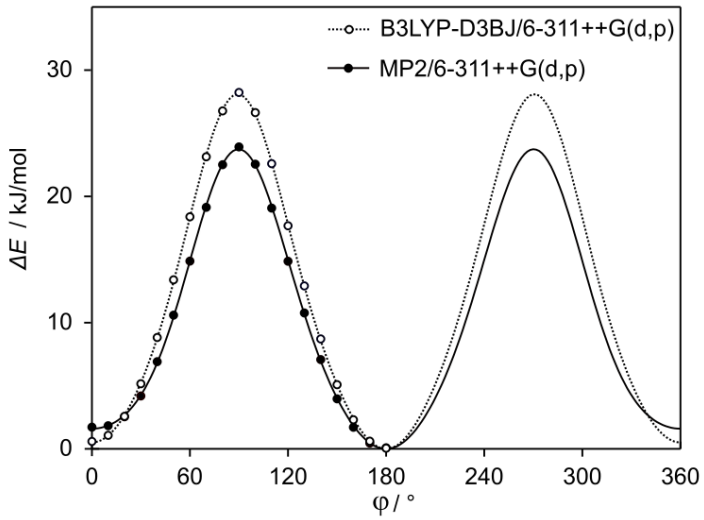

Figure 2: Potential energy curves of *E*-3-penten-2-one calculated by varying the dihedral angle φ = $\angle(O_6,C_5,C_7,C_9)$ in steps of 10° while optimizing all other geometries parameters at the B3LYP-D3BJ/6-311++G(d,p) level (dotted curve) and the MP2/6-311++G(d,p) level. Two minima are found, one at 0° (synperiplanar) and one at 180° (antiperiplanar).

Table 1: Rotational constants, dipole moment components, and optimized dihedral angle $\varphi = \angle(O_6,C_5,C_7,C_9)$ of the antiperiplanar (*ap*) and synperiplanar (*sp*) conformers of 3-penten-2-one calculated at the MP2/6-311++G(d,p) and B3LYP-D3BJ/6-311++G(d,p) levels of theory. The experimental rotational constants were obtained from the *2Tops* fit (see Section 3.2.).

	ap			***sp***		
Parameter	**MP2**	**B3LYP**	**Exp.**	**MP2**	**B3LYP**	**Exp.**
A / MHz	8328.1	8380.3	8369.6	9071.2	9156.8	9158.2
B / MHz	1910.2	1914.0	1914.1	1856.9	1861.5	1862.4
C / MHz	1584.4	1588.7	1589.6	1571.4	1577.0	1578.2
$\lvert\mu_a\rvert$ / D	3.47	3.33		1.80	1.80	
$\lvert\mu_b\rvert$ / D	2.90	2.40		3.01	2.67	
$\lvert\mu_c\rvert$ / D	0.00	0.00		0.00	0.00	
φ / °	180.0	180.0		0.0	0.0	

2.2. Basis set variation

For benchmarking purposes, geometry optimizations were repeated for the *ap* and *sp* conformer using different combinations of methods and basis sets. The calculated rotational constants and energies with or without zero-point corrections are summarized in Table S-3 in the Supplementary Material. It should be noted that the energetic order of the two conformers changes depending on the level of theory in use and whether zero-point corrections are applied or not, as given in Table 2. Therefore, it is not clear whether the *ap* or the *sp* conformer is energetically more favorable. As can be recognized from Figure 2 and Table 2, the energy difference is much larger in calculations at the MP2/6-311++G(d,p) level than in those at the B3LYP-D3BJ/6-311++G(d,p) level. In general, we observed a difference of about 2 kJ mol^{-1} or less. Eventually, both conformers have been identified in the microwave spectrum (see Section 3.2.).

Table 2: Absolute energies of the two conformers of 3-penten-2-one without (*E*) and with zero-point corrections (E_{ZPE}) calculated using different methods in combination with the 6-311++G(d,p) basis set. The energy difference between the *ap* and the *sp* conformers (*rel*) refers to $E_{ap} - E_{sp}$.

	***E* / Hartree**		$E_{(rel)}$ / kJ·mol^{-1}	E_{ZPE} / Hartree		$E_{ZPE(rel)}$ / kJ·mol^{-1}
Method	***ap***	***sp***		***Ap***	***sp***	
MP2	−269.832893	−269.832273	–1.63	−269.714657	−269.714356	–0.79
B3LYP-D3	−270.646706	−270.646682	–0.06	−270.529477	−270.529745	0.71
B3LYP-D3BJ	−270.656589	−270.656383	–0.54	−270.539441	−270.539470	0.08
CAM-B3LYP-D3BJ	–270.498217	–270.498440	0.59	–270.379839	–270.380273	1.14
M06-2X	−270.503615	−270.503436	–0.47	−270.385100	−270.385196	0.25
wB97X-D	–270.535833	–270.536641	2.12	–270.417437	–270.418573	2.98

2.3. Internal rotation

3-Penten-2-one features two methyl groups functioning as internal rotors, the acetyl methyl group **CH$_3$**–(C=O)– and the propenyl methyl group –CH=CH–**CH$_3$**. Since the two methyl groups are inequivalent, each rotational transition splits into five torsional species labelled as ($\sigma_1\sigma_2$) = (00), (01), (10), (11), and (12) [19], with the numbers 0, 1, 2 being equivalent to the three symmetry species A, E_a, E_b of the C_3 group [6]. σ_1 refers to the acetyl methyl group and σ_2 to the propenyl methyl group.

To predict the barrier to internal rotation of the acetyl methyl group, the dihedral angle α_1 was varied in steps of 10°, while a range of 120° was sufficient due to the symmetry of the methyl group. All other geometry parameters were optimized at the MP2/6-311++G(d,p) level of theory. The resulting energies were parametrized with a one-dimensional Fourier expansion. The potential energy curves of both conformers are depicted in Figure 3. For the propenyl methyl group, the same procedure was applied to the dihedral angle α_2 with the respective potential energy curves also illustrated in Figure 3.

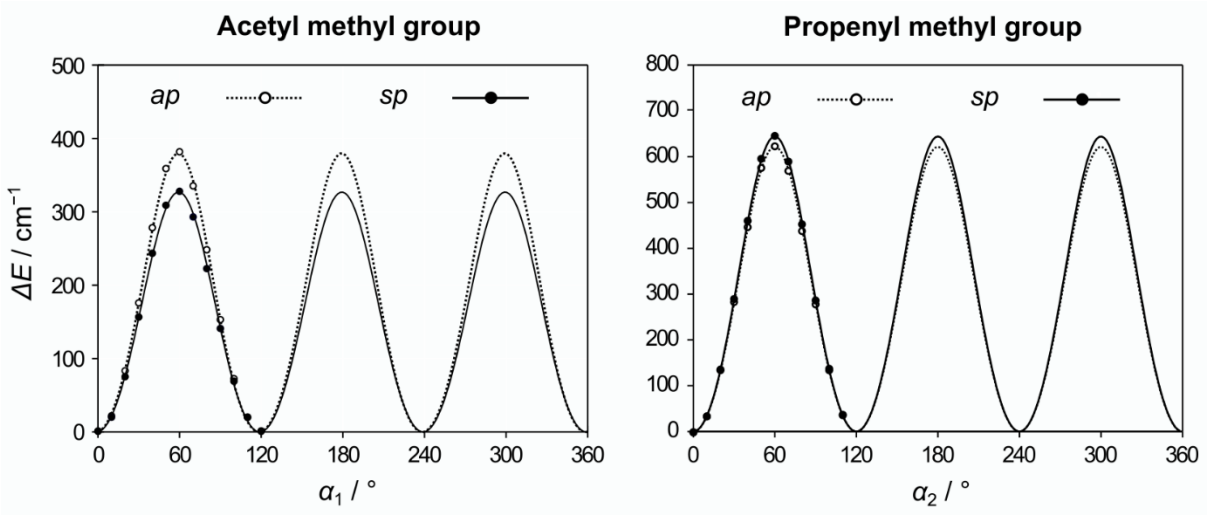

Figure 3: Potential energy curves calculated at the MP2/6-311++G(d,p) level of theory by rotating the acetyl and the propenyl methyl groups of the antiperiplanar (*ap*) and synperiplanar (*sp*) conformers of 3-penten-2-one. The energies are given relative to the lowest energy conformations with E = −269.832893 Hartree for the *ap* conformer and E = −269.832273 Hartree for the *sp* conformer.

As expected, the potential energy curves of both methyl groups show a threefold shape for both conformers. Similar to the potential energy curves given in Figure 2, we used a Fourier expansion with the terms given in Table S-4 of the Supplementary Material to parameterize the calculated energy points. Only a small V_6 contribution is necessary for the parameterization. In addition, a sine contribution is needed for the acetyl methyl group to reach a satisfactorily small maximal deviation within the dynamic range. The barrier height is between 300 cm^{-1} and 400 cm^{-1} for the acetyl methyl group and at about 650 cm^{-1} for the propenyl methyl group. Calculations are repeated at other levels of theory listed in Table 2, and the results are shown in Table 3. The values predicted for the propenyl methyl group are lower than the experimental value with a quite consistent discrepancy of less than 10%, while those predicted for the acetyl methyl group are higher and differ by up to 35% from the experimental value. On the one hand, extensive benchmarking on geometry optimizations exists, which helps to calculate reliable rotational constants and to guide the spectral assignment in many cases. On the other hand, it is still challenging to accurately calculate energies. Though from a quantum chemical point of view, an accuracy of 1 $kJ \cdot mol^{-1}$, corresponding to 84 cm^{-1}, already is a small error for energy calculations, it does not meet the experimental requirements of microwave spectroscopy, where a change of one cm^{-1} in the potential barrier might lead to a shift of hundreds of MHz of the

frequencies. Currently, benchmarking on barriers to internal rotations does not exist in the literature. However, there is an on-going study for ketones containing an acetyl methyl group, showing that the combination CCSD/cc-pVTZ//B3LYP-D3/cc-pVTZ yields quite accurate values for the barrier heights [20]. CCSD energy point calculations are performed on the B3LYP-D3 optimized minimum geometry and on the transition state. The difference corresponds to the barrier height. Applying this method, we found a barrier of 415.1 cm^{-1} for the *ap* conformer and 362.9 cm^{-1} for the *sp* conformer.

Table 3: Barriers to internal rotation (in cm^{-1}) of the acetyl methyl and the propenyl methyl groups of the two conformers *ap* and *sp* of 3-penten-2-one calculated with different methods in combination with the 6-311++G(d,p) basis set. The experimental values (Exp.) are obtained from the *2Tops* fit (see Section 3.2.). The deviations between the experimental and the calculated values are given as absolute values (in cm^{-1}), as well as in percent relative to the experimental values in parentheses.

	ap				***sp***			
Method	**Acetyl**	**Dev.**	**Propenyl**	**Dev.**	**Acetyl**	**Dev.**	**Propenyl**	**Dev.**
MP2	379.9	54 (12)	621.5	–40 (7)	325.8	32 (9)	644.2	–49 (8)
B3LYP-D3	302.7	131 (30)	614.8	–33 (6)	280.7	77 (22)	644.0	–49 (8)
B3LYP-D3BJ	282.2	152 (35)	618.8	–37 (6)	270.1	88 (25)	647.5	–52 (9)
CAM-B3LYP-D3BJ	307.1	127 (29)	623.0	–41 (7)	284.7	73 (20)	651.7	–56 (9)
M06-2X	431.1	3 (1)	619.5	–38 (6)	325.1	33 (9)	648.5	–53 (9)
wB97X-D	355.1	79 (18)	600.6	–19 (3)	287.9	70 (20)	630.0	–35 (6)
Exp.	**434.1**		**581.9**		**358.1**		**595.3**	

To study the coupling of the two methyl torsions, we also calculated the two-dimensional (2D) potential energy surface (PES) by varying the dihedral angles α_1 and α_2 in a grid of 10° and optimizing all other geometry parameters at the MP2/6-311++G(d,p) and the B3LYP-D3BJ/6-311++G(d,p) levels. The energy data points were parameterized with a 2D-Fourier expansion given in Table S-5 of the Supplementary Material, which were used to draw the PES as a color contour plot given in Figure 4. In addition to the cos(3nα) terms, the coupling terms $sin(3\alpha_1) \cdot sin(3\alpha_2)$ and $cos(3\alpha_1) \cdot cos(3\alpha_2)$ are used for the parameterization, while the former has a much larger value than the latter.

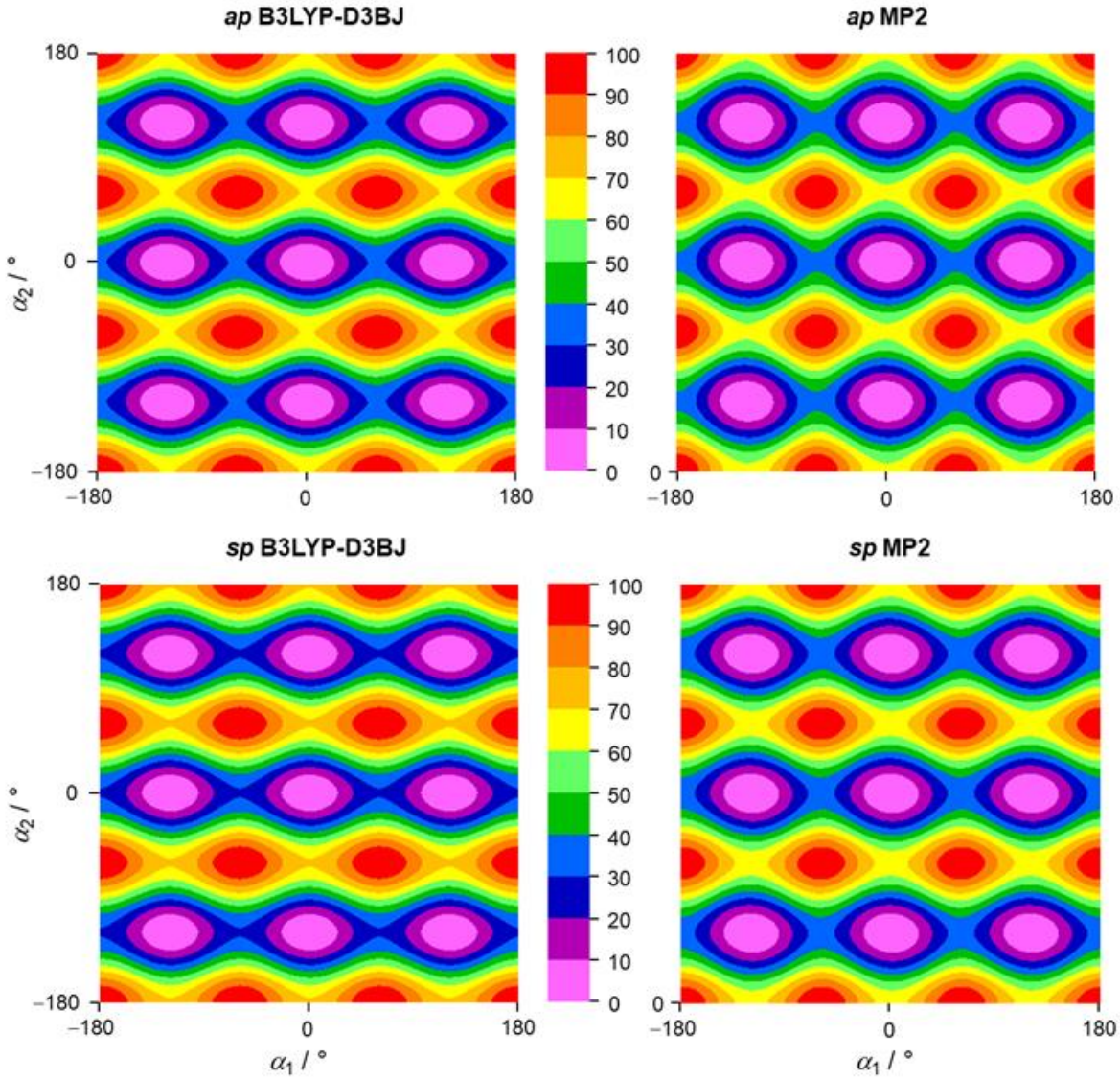

Figure 4: Potential energy surfaces of the antiperiplanar (*ap*) and synperiplanar (*sp*) conformer of 3-penten-2-one calculated with the B3LYP-D3BJ and MP2 methods in combination with the 6-311++G(d,p) basis set by varying the dihedral angles α_1 = ∠(O_6,C_5,C_1,H_3) and α_2 = ∠(C_7,C_9,C_{11},H_{12}). The numbers in the color code indicate the energy in percent with respect to the lowest energy conformations (0%) at E_{ap} = −270.656589 Hartree with the B3LYP-D3BJ method and −269.832894 Hartree with the MP2 method as well as the highest energy conformations (100%) at −270.652495 and −269.828316 Hartree, respectively. The respective minimum values for the *sp* conformer are −270.656383 and −269.832273 Hartree, and the respective maximum values are −270.652181 and −269.827806 Hartree.

3. Microwave spectrum

3.1. Experimental setup

The microwave spectrum of 3-penten-2-one was measured using a molecular jet Fourier transform microwave spectrometer operating in the frequency range from 2.0 to 26.5 GHz [21]. The substance was purchased from Sigma Aldrich, Merck KGaA, Darmstadt, Germany, as a mixture of the *E* and the *Z* isomers with a stated purity of ≥ 95% and no further purification steps were carried out. 3-Penten-2-one was put on a piece of a pipe cleaner placed in a steel tube in front of the nozzle and expanded in the Fabry-Pérot resonator under a helium flow through the tube with a pressure of about 200 kPa. A scan of overlapping spectra with a step width of 0.25 MHz was recorded from 9.0 GHz to 14.7 GHz. After the first assignment, high resolution measurements within the operating frequency range of the spectrometer were performed. In this mode, an experimental accuracy of about 2 kHz can be achieved [22].

3.2. Spectral assignment

To assign the recorded survey spectrum, 3-penten-2-one was initially considered as a rigid rotor and the rotational constants calculated at the MP2/6-311++G(d,p) level of theory given in Table 1 were inserted into the *XIAM* code [23] to predict a theoretical spectrum. By comparing the calculated and experimental spectra, transitions of both conformers could be assigned straightforwardly. However, fitting them with frequencies measured at high resolution using a standard rigid-rotor model led to standard deviations between 300 kHz and 500 kHz, more than a hundred times the experimental accuracy (2 kHz). The inclusion of centrifugal distortion constants did not improve the situation. The reason for this problem can be traced back to the splittings caused by the internal rotations of the acetyl methyl and propenyl methyl group, with torsional barrier values being the same order of magnitude (see Section 2.3.). The scale of the splittings between the five torsional species ranges from a few MHz down to a few kHz. In some cases, the splittings are not resolvable. Moreover, each branch shows its unique splitting pattern. An example is given in Figure 5 for the $4_{13} \leftarrow 3_{12}$ transition of the *ap* conformer of 3-penten-2-one. The spectral features also change significantly if barrier heights calculated at different levels of theory (see Table 3) are used as initial values for the prediction. Therefore, although the rotational quantum numbers were assigned well in the first fitting attempts, the (00) species had not been correctly identified because one of other torsional species (01), (10), (11), or (12) was taken into the fit. In some cases, they appear in the same high resolution

measurement (as can be seen in Figure 5) and the intensity of each species is not a good reference to ease the assignment, since it is mainly depending on the polarization frequency.

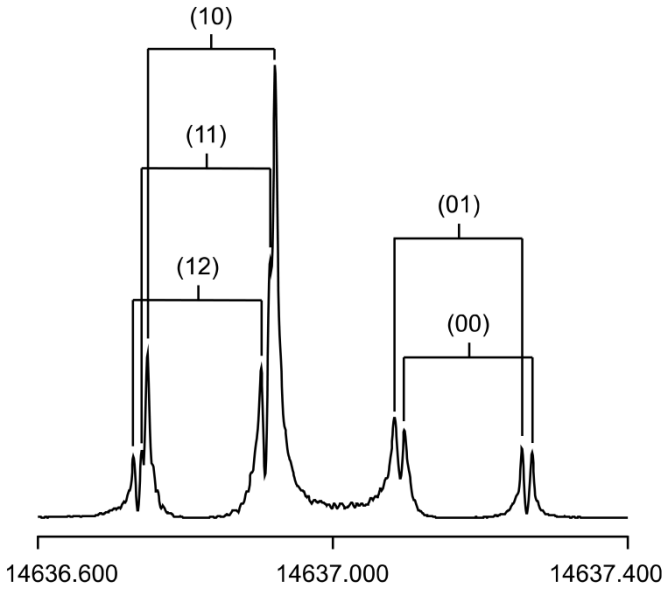

Figure 5: A typical high resolution measurement of the $4_{13} \leftarrow 3_{12}$ transition of the antiperiplanar (*ap*) conformer of 3-penten-2-one. The frequencies are given in MHz, with the (00), (01), (10), (11), and (12) species found at 14637.1844 MHz, 14637.1719 MHz, 14636.8355 MHz, 14636.8291 MHz, and 14636.8172 MHz, respectively. The splittings indicated with the brackets are caused by the Doppler effect.

Due to a lack of reliable starting values for the barriers, multiple cycles of trial and error were necessary to assign the torsional species. We note that there are other techniques to assign spectra, such as using combination difference loops [24], or fitting the torsional species separately [11,25-27]. But, for 3-penten-2-one, it worked best to switch between different *XIAM* fits floating various sets of parameters. Fits including only the (00) species using a (semi-)rigid rotor model will be referred to as *0Top*. Fits *1Top Acetyl* and *1Top Propenyl* consider either the (00) and (10) or the (00) and (01) species lines, respectively. The *2Tops* fits include all torsional species lines and treat the internal rotation of both rotors simultaneously. Eventually, standard deviations in agreement with the experimental accuracy could be achieved in global fits for both conformers, proving the assignments to be correct. The fits are presented in Tables 4 and 5, the frequency lists in Tables S-6 and S-7 in the Supplementary Material. In all *1Top* and *2Tops* fits, the rotational constants F_0 of both methyl groups were fixed to 158 GHz, a value

often found for methyl tops, due to correlation with the V_3 parameters. Furthermore, though quantum chemical calculations suggest a significant value for the $sin(3\alpha_1) \cdot sin(3\alpha_2)$ coupling term (see Section 2.3 and Table S-5 of the Supplementary Material), the corresponding V_{ss} fitting parameter available in *XIAM* is not required to achieve satisfactory fits for both conformers.

Table 4: Molecular parameters of the *ap* conformer of 3-penten-2-one obtained from the *XIAM* program. Fit *0Top* considers only the (00) species lines. Fit *1Top Acetyl* includes the (00) and (10) and Fit *1Top Propenyl* the (00) and (01) species. Fit *2Tops* takes all torsional species lines into account.

Par.[a]	**Unit**	***0Top***	***1Top Acetyl***	***1Top Propenyl***	***2Tops***	**Calc.**[b]
A	MHz	8368.81945(36)	8368.73666(25)	8368.63701(25)	8368.55439(16)	8267.557
B	MHz	1914.141708(77)	1914.108065(63)	1914.170024(60)	1914.136437(43)	1892.780
C	MHz	1588.62570(11)	1588.620400(80)	1588.596450(77)	1588.591079(54)	1570.949
Δ_J	kHz	0.13255(74)	0.13226(56)	0.13282(52)	0.13212(36)	0.12724
Δ_{JK}	kHz	1.9029(49)	1.8962(39)	1.8980(34)	1.8898(26)	1.88378
Δ_K	kHz	2.789(30)	2.805(22)	2.607(21)	2.642(14)	2.49762
δ_J	kHz	0.02447(23)	0.02426(17)	0.02405(16)	0.02414(11)	0.02331
δ_K	kHz	1.044(16)	1.020(12)	1.0430(11)	1.0245(75)	0.97152
$V_{3,1}$	cm^{-1}		434.136(56)		434.149(37)	415.1
$\angle(i_1,a)$[c]	°		108.445(12)		108.4486(80)	103.026
$\angle(i_1,b)$	°		18.445(12)		18.4486(80)	13.026
$D_{pi2-,1}$	MHz		−0.0749(22)		−0.0741(15)	
$V_{3,2}$	cm^{-1}			581.875(67)	581.903(45)	621.5
$\angle(i_2,a)$[c]	°			17.986(78)	17.951(53)	16.728
$\angle(i_2,b)$	°			107.986(78)	107.951(53)	106.728
N[d]		97	200	200	505	
$N_{(00)/(10)/(01)}$[e]		97/0/0	97/103/0	97/0/103	97/103/103	
$N_{(11)/(12)}$[f]		0/0	0/0	0/0	99/103	
σ[g]	kHz	2.6	2.7	2.6	2.7	

[a] All parameters refer to the principal axis system. Watson's A reduction and I^r representation were used. [b] Calculated at the MP2/6-311++G(d,p) level of theory except for the $V_{3,1}$ value which is obtained at the CCSD/cc-pVTZ//B3LYP-D3/cc-pVTZ level (see text). Ground state rotational constants are given. The centrifugal distortion constants were obtained by anharmonic frequency calculations. [c] For both rotors, $\angle(i,c)$ was fixed to 90° due to symmetry. [d] Total number of lines. [e] Number of the (00)/(10)/(01) species lines, respectively. [f] Number of the (11)/(12) species lines, respectively. [g] Standard deviation of the fit.

Table 5: Molecular parameters of the *sp* conformer of 3-penten-2-one obtained from the *XIAM* program. Fit *0Top* considers only the (00) species lines. Fit *1Top Acetyl* includes the (00) and (10) and Fit *1Top Propenyl* the (00) and (01) species. Fit *2Tops* takes all torsional species lines into account.

Par.[a]	**Unit**	***0Top***	***1Top Acetyl***	***1Top Propenyl***	***2Tops***	**Calc.**[b]
A	MHz	9160.24109(48)	9158.39633(88)	9160.04917(34)	9158.20427(56)	8983.919
B	MHz	1862.41765(16)	1862.39767(15)	1862.44624(12)	1862.426431(94)	1845.096
C	MHz	1578.25363(22)	1578.22604(18)	1578.22407(16)	1578.19645(11)	1564.357
Δ_J	kHz	0.1282(12)	0.12686(90)	0.12843(85)	0.12783(56)	0.12270
Δ_{JK}	kHz	1.813(12)	1.7015(86)	1.8016(84)	1.6903(53)	1.73343
Δ_K	kHz	9.394(68)	8.207(65)	9.227(51)	8.070(43)	7.22214
δ_J	kHz	0.02144(25)	0.02144(19)	0.02144(18)	0.02158(12)	0.02087
δ_K	kHz	0.890(70)	0.842(58)	0.893(51)	0.851(37)	0.54308
$V_{3,1}$	cm^{-1}		357.278(40)		358.076(26)	362.9
$\angle(i_1,a)$[c]	°		141.732(28)		141.749(17)	138.342
$\angle(i_1,b)$	°		128.268(28)		128.252(17)	131.658
$D_{pi2-,1}$	MHz		−0.0302(15)		−0.03052(95)	
$D_{pi2K,1}$	MHz		−0.644(30)		−0.635(19)	
$V_{3,2}$	cm^{-1}			593.89(11)	595.271(71)	644.2
$\angle(i_2,a)$[c]	°			20.30(11)	20.152(69)	19.322
$\angle(i_2,b)$	°			110.30(11)	110.152(69)	109.322
N[d]		72	159	150	410	
$N_{(00)/(10)/(01)}$[e]		72/0/0	72/87/0	72/0/78	72/87/78	
$N_{(11)/(12)}$[f]		0/0	0/0	0/0	86/87	
σ[g]	kHz	2.6	2.8	2.7	2.7	

[a] All parameters refer to the principal axis system. Watson's A reduction and I^r representation were used. [b] Calculated at the MP2/6-311++G(d,p) level of theory except for the $V_{3,1}$ value which is obtained at the CCSD/cc-pVTZ//B3LYP-D3/cc-pVTZ level (see text). Ground state rotational constants are given. The centrifugal distortion constants were obtained by anharmonic frequency calculations. [c] For both rotors, $\angle(i,c)$ was fixed to 90° due to symmetry. [d] Total number of lines. [e] Number of the (00)/(10)/(01) species lines, respectively. [f] Number of the (11)/(12) species lines, respectively. [g] Standard deviation of the fit.

4. Discussion

4.1. Geometry parameters

Two conformers with C_s symmetry were assigned in the microwave spectrum of 3-penten-2-one. Theoretically, it is not clear whether the *ap* or the *sp* conformer is the energetically more favorable structure, since the energy order changes depending on the level of theory in use, as mentioned in Section 2.2. Experimentally, the line intensities of the survey spectrum recorded under the measurement conditions described in Section 3.1. are not reliable to deduce the population ratio. Furthermore, Stark measurements are not available to yield experimental confirmation to the predicted dipole moment components given in Table 1 with a μ_a^2/μ_b^2 ratio

of 1.4 (MP2 calculations) for the *ap* conformer compared to 0.4 for the *sp* conformer. Quantitative statements are not attempted, but qualitatively, both conformers seem to be equally present in the spectrum. Some other molecules exhibiting a double bond in the α,β-position of a carbonyl group, such as acrolein [28], methacrolein [29], and crotonaldehyde [30,31], show a clear preference for the conformer equivalent to the *ap* conformer of 3-penten-2-one. For methyl vinyl ketone, Zakharenko et al. determined a population ratio N_{ap}/N_{sp} of 2.2 [32]. Nevertheless, in the case of methyl methacrylate [33], the energetic difference between the two conformers is very small, and for methacrylate [34] only the equivalent to the *sp* conformer has been assigned.

The rotational constants obtained from different fits of one conformer (see Tables 4 and 5, respectively) are in good agreement, but they do not coincide within their respective errors. It is known that by fitting only the (00) species lines as in Fit *0Top*, or the (00) lines with either the (01) or the (01) species as in Fit *1Top*, the rotational constants become effective and no longer represent structural parameters as they are in the global *2Tops* fit. Comparing the experimentally deduced rotational constants with those calculated at different levels of theory (see Section 2.2. and Table S-3 of the Supplementary Material), deviations of about 1% or less are observed for both conformers, which are sufficiently reliable for a good prediction of the microwave spectrum. We found excellent agreement for the rotational constants of the *ap* conformer calculated with the B3LYP-D3 and B3LYP-D3BJ methods in combination with the Pople's 6-311 basis set and the (d,p) polarization function, independent on the use of diffuse function. The wB97X-D functional in combination with Dunning's cc-pVDZ basis set with or without diffuse function (aug) also provides very satisfactory results. For the *sp* conformer, the combination of the B3LYP-D3BJ method, the 6-311 basis set, and the (d,p) polarization function as well as the combination of the wB97X-D method and the cc-pVDZ basis set also yield the best agreement, however, the use of diffuse function (+, ++, or aug) is necessary. Without Becke-Johnson damping, the B3LYP-D3 method performs well with the 6-311 basis set and the (df,pd) polarization function. Overall, regarding also the results for other molecules with a conjugated double bond system, such as 2,6- [25] and 3,4-dimethylfluorobenzene [26], or 2-acetylfuran [35], the B3LYP-D3BJ/6-311++G(d,p) level of theory yields X_e values of equilibrium rotational constants (with $X = A, B, C$), which are in almost exact agreement with the experimental X_0 values. It is obvious that from a theoretical perspective, the X_e constants should not be compared with the X_0 constants. However, error compensations could be benefited to access good starting values of the rotational constants for the assignment guidance.

This often works well for a certain class of molecules and has become a common way in the experimental practice. Error compensations also explain why diffuse functions are needed for one conformer (*ap*) but not for the other (*sp*).

4.2. The "mesomeric class"

According to the *2Tops* fits shown in Tables 4 and 5, the experimentally deduced barriers to internal rotation are 434.149(37) cm^{-1} for the acetyl methyl group and 581.903(45) cm^{-1} for the propenyl methyl group in the case of the *ap* conformer. For the *sp* conformer, they are 358.076(26) cm^{-1} and 595.271(71) cm^{-1}, respectively. Considering the classification system described in the introduction, the barrier heights of the acetyl methyl torsion of 3-penten-2-one fit in the "mesomeric class", containing molecules with a double bond in the α,β-position, which is conjugated to the carbonyl group. As illustrated in Figure 6, this class also encloses methyl vinyl ketone [16] and ionone [17], and contains two sub-classes. Antiperiplanar (*ap*) conformers feature barriers of about 430 cm^{-1}, while the barriers in synperiplanar (*sp*) conformers are approximately 350 cm^{-1}. The *sp* conformer of acetyl isocyanate [36] also fits perfectly in the "mesomeric class", showing that the presence of a nitrogen atom in the conjugated system does not affect the barrier height. The higher value found for the *ap* conformers might be explained by steric hindrance, since the double bond is located closer to the acetyl methyl group than in the *sp* conformation. During the internal rotation, the acetyl methyl group seems to be able to sense the π-conjugated system on the other side of the carbonyl group. Interestingly, this sensor ability appears to end at the α,β-double bond, as can be recognized in α-ionone and β-ionone where a bulky six-membered ring is attached to the β-carbon [17]. In β-ionone, the conjugated π-system is extended with the double bond of the ring [17], but neither the ring conformation, nor the extension of the conjugated double bonds seem to influence the torsional barrier of the acetyl methyl group in either conformer. This has also been reported in the cases of acetates, where the acetyl methyl torsion is hindered by the same barrier of about 150 cm^{-1} in both vinyl acetate [37] and butadienyl acetate [38].

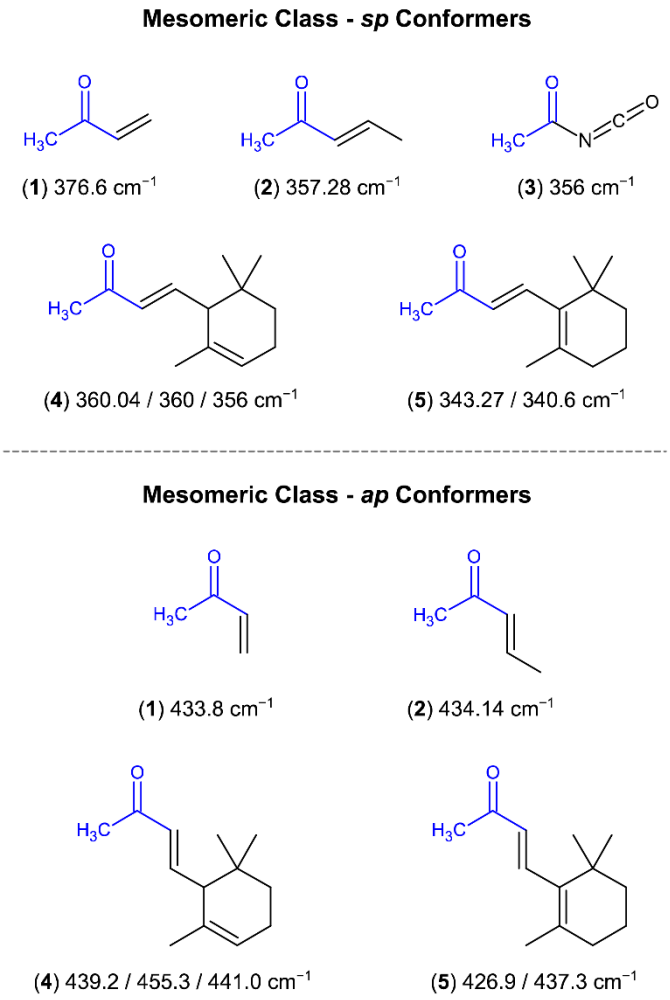

Figure 6: Ketones of the "mesomeric class" and the respective barrier height of the acetyl methyl group: (**1**) methyl vinyl ketone [16], (**2**) 3-penten-2-one (this work), (**3**) acetyl isocyanate [36], (**4**) α-ionone [17] and (**5**) β-ionone [17]. For ionone, various values are given for the barrier height, referring to different conformations of the ring (see Ref. [17]).

4.3. Propenyl methyl torsion

The barrier to the internal rotation of the propenyl methyl group is 581.903(45) cm^{-1} and 595.271(71) cm^{-1} for the *ap* and *sp* conformer, respectively. They are of the same order of magnitude as the barrier heights found for the propenyl methyl or isopropenyl methyl groups of propene (698.4 cm^{-1}) [39], isopropenyl acetate (711.7(73) cm^{-1}) [40], and crotonaldehyde (about 606 cm^{-1}) [30,31], as well as methacrolein (491.574(24) cm^{-1}) [29] and methyl methacrylate (632.5(73) cm^{-1} for the *ap* conformer and 761.7(87) cm^{-1} for the *sp* conformer) [33]. In general, methyl groups attached to double bonds show barrier heights ranging from

approximately 500 cm^{-1} to 750 cm^{-1}. This is much smaller than the values of about 1000 cm^{-1} found for methyl groups at the end of an alkyl chain [10,41,42]. We suspect the orbital interactions to be the reason. However, benchmarking on barriers to methyl internal rotation is required to support any statement on this subject.

5. Conclusions

The antiperiplanar (*ap*) and the synperiplanar (*sp*) conformers were identified in the microwave spectrum of *E*-3-penten-2-one. The complicated splitting patterns arising due to the internal rotation of the acetyl methyl and the propenyl methyl group could be resolved and fitted to measurement accuracy, yielding barrier heights of 434.149(37) cm^{-1} and 358.076(26) cm^{-1} for the acetyl methyl group of the *ap* and *sp* conformers, respectively. This finding establishes the "mesomeric class" suggested in Ref. [10], which belongs to a systematic categorization aiming to connect the acetyl methyl torsion to structural aspects of ketones. For the propenyl methyl group, the barrier to internal rotation is 581.903(45) cm^{-1} for the *ap* conformer and 595.271(71) cm^{-1} for the *sp* conformer.

Acknowledgements

This work was supported by the Agence Nationale de la Recherche ANR (project ID ANR-18-CE29-0011). Simulations were performed with computing resources granted by the RWTH Aachen University under the projects rwth0249 and rwth0506.

References

[1] W. Gordy, R.L. Cook, *Microwave Molecular Spectra*, Vol. 18, 3rd Ed., Wiley: New York, USA, (1984).

[2] C.E. Cleeton, N.H. Williams, *Phys. Rev.* **45**, 234 (1934).

[3] H.V.L. Nguyen, I. Gulaczyk, M. Kręglewski, I. Kleiner, *Coord. Chem. Rev.* **436**, 213797 (2021).

[4] A. Legon, *Chem. Rev.* **80**, 231 (1980).

[5] H.V.L. Nguyen, I. Kleiner, *Phys. Sci. Rev.* **6** (2021), online. DOI: 10.1515/psr-2020-0037.

[6] H. Dreizler, *Z. Naturforsch.* **16a**, 1354 (1961).

[7] M. Andresen, I. Kleiner, M. Schwell, W. Stahl, H.V.L. Nguyen, *J. Phys. Chem. A* **122**, 7071 (2018).

[8] M. Andresen, I. Kleiner, M. Schwell, W. Stahl, H.V.L. Nguyen, *ChemPhysChem* **20**, 2063 (2019).

[9] M. Andresen, I. Kleiner, M. Schwell, W. Stahl, H.V.L. Nguyen, *J. Phys. Chem. A* **124**, 1353 (2020).

[10] M. Andresen, D. Schöngen, I. Kleiner, M. Schwell, W. Stahl, H.V.L. Nguyen, *ChemPhysChem* **21**, 2206 (2020).

[11] S. Herbers, S.M. Fritz, P. Mishra, H.V.L. Nguyen, T.S. Zwier, *J. Chem. Phys.* **152**, 074301 (2020).

[12] V.V. Ilyushin, J.T. Hougen, *J. Mol. Spectrosc.* **289**, 41 (2013).

[13] G.S. Grubbs II, P. Groner, S.E. Novick, S.A. Cooke, *J. Mol. Spectrosc.* **280**, 21 (2012).

[14] L. Evangelisti, L.B. Favero, A. Maris, S. Melandri, A. Vega-Toribio, A. Lesarri, W. Caminati, *J. Mol. Spectrosc.* **259**, 65 (2010).

[15] L. Tulimat, H. Mouhib, I. Kleiner, W. Stahl, *J. Mol. Spectrosc.* **312**, 46 (2015).

[16] D.S. Wilcox, A.J. Shirar, O.L. Williams, B.C. Dian, *Chem. Phys. Lett.* **508**, 10 (2011).

[17] I. Uriarte, S. Melandri, A. Maris, C. Calabrese, E.J. Cocinero, *J. Phys. Chem. Lett.* **9**, 1497 (2018).

[18] M.J. Frisch, G.W. Trucks, H.B. Schlegel, G.E. Scuseria, M.A. Robb, J.R. Cheeseman, G. Scalmani, V. Barone, G.A. Petersson, H. Nakatsuji, X. Li, M. Caricato, A.V. Marenich, J. Bloino, B.G. Janesko, R. Gomperts, B. Mennucci, H.P. Hratchian, J.V. Ortiz, A.F. Izmaylov, J.L. Sonnenberg, D. Williams-Young, F. Ding, F. Lipparini, F. Egidi, J. Goings, B. Peng, A. Petrone, T. Henderson, D. Ranasinghe, V.G. Zakrzewski, J. Gao, N. Rega, G. Zheng, W. Liang, M. Hada, M. Ehara, K. Toyota, R. Fukuda, J. Hasegawa, M. Ishida, T. Nakajima, Y. Honda, O. Kitao, H. Nakai, T. Vreven, K. Throssell, J.A. Montgomery, Jr., J. E. Peralta, F. Ogliaro, M.J. Bearpark, J.J. Heyd, E.N. Brothers, K.N. Kudin, V.N. Staroverov, T.A. Keith, R. Kobayashi, J. Normand, K. Raghavachari, A.P. Rendell, J.C. Burant, S.S. Iyengar, J. Tomasi, M. Cossi, J.M. Millam, M. Klene, C. Adamo, R. Cammi, J.W. Ochterski, R.L. Martin, K. Morokuma, O. Farkas, J.B. Foresman, D.J. Fox, Gaussian 16, Revision B.01, Inc., Wallingford CT, 2016.

[19] L. Ferres, J. Cheung, W. Stahl, H.V.L. Nguyen, *J. Phys. Chem. A* **123**, 3497 (2019).

[20] K.G. Lengsfeld, P. Buschmann, private communication.

[21] J.-U. Grabow, W. Stahl, H. Dreizler, *Rev. Sci. Instrum.* **67**, 4072 (1996).

[22] J.-U. Grabow, W. Stahl, *Z. Naturforsch.* **45a**, 1043 (1990).

[23] H. Hartwig, H. Dreizler, *Z. Naturforsch.* **51a**, 923 (1996).

[24] Y. Zhao, H.V.L. Nguyen, W. Stahl, J.T. Hougen, *J. Mol. Spectrosc.* **318**, 91 (2015).

[25] S. Khemissi, H.V.L. Nguyen, *ChemPhysChem* **21**, 1682 (2020).

[26] J. Mélan, S. Khemissi, H.V.L. Nguyen, *Spectro. Chim. Acta A* **253**, 119564 (2021).

[27] N. Ohashi, J.T. Hougen, R.D. Suenram, F.J. Lovas, Y. Kawashima, M. Fujitake, J. Pykad, *J. Mol. Spectrosc.* **227**, 28 (2004).

[28] C.E. Blom, G. Grassi, A. Bauder, *J. Am. Chem. Soc.* **106**, 7427 (1984).

[29] O. Zakharenko, R.A. Motiyenko, J.-R. Aviles Moreno, A. Jabri, I. Kleiner, T.R. Huet, *J. Chem. Phys.* **144**, 024303 (2016).

[30] S.L. Hsu, W.H. Flygare, *Chem. Phys. Lett.* **4**, 317 (1969).

[31] M. Suzuki, K. Kozima, *Bull. Chem. Soc. Jpn* **42**, 2183 (1969).

[32] O. Zakharenko, R.A. Motiyenko, J.R. Aviles Moreno, T.R. Huet, *J. Phys. Chem. A* **121**, 6420 (2017).

[33] S. Herbers, D. Wachsmuth, D.A. Obenchain, J.-U. Grabow, *J. Mol. Spectrosc.* **343**, 96 (2018).

[34] G. Williams, N.L. Owen, J. Sheridan, *Trans. Faraday Soc.* **67**, 922 (1971).

[35] C. Dindić, A. Lüchow, N. Vogt, J. Demaison, H.V.L. Nguyen, *J. Phys. Chem. A* **125**, 4986 (2021).

[36] B.M. Landsberg, K. Iqbal, *J. Chem. Soc. Faraday Trans.* **76**, 1208 (1980).

[37] H.V.L. Nguyen, A. Jabri, V. Van, W. Stahl, *J. Phys. Chem. A* **118**, 12130 (2014).

[38] A. Jabri, V. Van, H.V.L. Nguyen, W. Stahl, I. Kleiner, *ChemPhysChem* **17**, 2660 (2016).

[39] E. Hirota, *J. Chem. Phys.* **45**, 1984 (1966).

[40] H.V.L. Nguyen, W. Stahl, *J. Mol. Spectrosc.* **264**, 120 (2010).

[41] L. Tulimat, H. Mouhib, H.V.L. Nguyen, W. Stahl, *J. Mol. Spectrosc.* **373**, 111356 (2020).

[42] K.J. Koziol, W. Stahl, H.V.L. Nguyen, *J. Chem. Phys.* **153**, 184308 (2020).